J Mol Model (2010) 16:489–498
DOI 10.1007/s00894-009-0561-7

ORIGINAL PAPER

Simulation of structural and functional properties of mevalonate diphosphate decarboxylase (MVD)

Samantha Weerasinghe · Ranil Samantha Dassanayake

Received: 19 March 2009 / Accepted: 4 July 2009 / Published online: 4 August 2009

Abstract Mevalonate 5-diphosphate decarboxylase (MVD) is an important enzyme in the mevalonate pathway catalyzing the ATP-dependent decarboxylation of mevalonate 5-diphosphate (MDP) to yield isopentynyl diphosphate (IPP) which is an ubiquitous precursor for isoprenoids and sterols. Although there are studies to show the involvement of certain amino acid residues in MVD activity, the structure and the function of the active site is yet to be investigated. Therefore the objectives of this study were to elucidate the active site of *Saccharomyces cerevisiae* MVD (scMVD) using a molecular docking and simulation-based approach. The Cartesian coordinates of scMVD retrieved from the PDB database were used in the docking procedure. 3D atomic coordinates of MDP, ATP and an inhibitor trifluoromevalonate (TFMDP) were generated using Gaussian 98. ATP, MDP and TFMDP were docked into the potential active site identified by sequence analyses using Hex 4.2. The complexes obtained from docking procedure were subjected to 1.5 ns simulation by GROMACS 3.2. Investigation of complexes revealed that Ala15, Lys18, Ser121 & Ser155; Lys22, Ser153 & Ser155 and Tyr19, Ser121, Ser153, Gly154 & Thr209 of MVD are within hydrogen bond forming distances of MDP, ATP and TFMDP, respectively indicating their possible involvement in active site formation through H-bond formation. The presence of a water molecule between the carboxyl group of Asp302, a previously characterized active site residue and C3 region of MDP at a distance of 3 Å suggests that deprotonation of the hydroxyl of the C3 takes place *via* a water molecule. Conjunction with reported crucial catalytic activity of Ser121 of MVD and our finding of the presence of this residue in hydrogen bond forming distance to MDP suggests that this hydrogen bond helps in proper orienting of MDP for phosphorylation /decarboxylation. We further suggest that the reported greater RMS deviation of Pro_{79}-Leu mutated MVD with respect to native MVD of temperature sensitive mutant phenotype of *S. cerevisiae* is due to partial unfolding of MVD as a result of mutation. Finally, this study provides a tantalizing glimpse about hitherto unknown structural and functional properties of the active site of MVD.

Keywords Mevalonate 5-diphosphate decarboxylase · Molecular docking · Molecular simulation

S. Weerasinghe · R. Samantha Dassanayake (✉)
Department of Chemistry, Faculty of Science,
University of Colombo,
Colombo 00300, Sri Lanka
e-mail: rsdassan@webmail.cmb.ac.lk

Introduction

Isopentenyl pyrophosphate (IPP) and dimethylallyl pyrophosphate (DMAPP) are key building blocks of a large family of fundamental biomolecules. Two distinct biosynthetic pathways, the mevalonate (MVA) pathway [1, 2] and the non-mevalonate, known as 2-*C*-methyl-D-erythritol 4-phosphate/1-deoxy-D-xylulose 5-phosphate pathway [3, 4] synthesize IPP and DMAPP. The MVA pathway is present in all higher eukaryotes, archaea, a few eubacteria, the cytosol and mitochondria of plants, fungi, and *Trypanosoma* and *Leishmania* [5] while the non-mevalonate pathway is present in plants chloroplasts, algae, cyanobacteria and in apicomplexan protozoa such as the malaria parasite where this pathway takes place in their plastids [3, 6–8]. In addition, most eubacteria including important pathogens such as *Mycobacterium tuberculosis* synthesize IPP and DMAPP *via* the non-mevalonate pathway [9]. IPP

and DMAPP are precursors for numerous biomolecules such as sterols, isoprenoids, dolichols, side chain of ubiquinone, prenyl group of prenylated proteins, isopentenyl adenine present in some transfer RNAs, intracellular messengers such as cytokines in plants, chlorophyll, caretenoids and farnesylated mating factors in fungi [5, 10–13] indicating the essentiality of MVD in cell viability [14]. Sterols are one of the major structural components of the cell membrane which play a role in cell permeability, activity of membrane bound enzymes, hormone binding to membranes *etc*. Isoprenoids are essential in signal transduction processes. Dolichol is involved in the synthesis of glycoproteins while ubiquinone is involved in electron transport in the mitochondrial chain. In mammalian and yeast cells isoprenylated proteins are involved in mitogenic signal transduction [5, 10].

Mevalonate diphosphate decarboxylase (MVD) is a unique enzyme in mevalonate biosynthetic pathway that catalyses the divalent ion dependent decarboxylation of mevalonate 5-diphosphate (MDP/ Fig. 1a) to isopentynyl diphosphate (IPP), with concurrent hydrolysis of ATP to form ADP and inorganic phosphate [15]. MVD belongs to the GHMP kinase domain superfamily and is one of the least studied enzymes in this family. The genes that encode MVD have been cloned and characterized from evolutionally diverse organisms. The functions of *Saccharomyces cerevisiae* (ScMDD) [14], primitive eukaryotes *Trypanosoma brucei* (tbMDD), *prokaryotic Staphylococcus aureus* (SaMDD) [16] *Candida albicans* (caMVD) [17] and *Arabidopsis thaliana* [18] have been demonstrated using yeast complementation assays of the temperature sensitive phenotype. To date, only a few crystal structures of ScMDD, tbMDD and SaMDD are available in the PDB database all of which are unliganded [16, 19]. Mutagenesis followed by kinetic studies has shown the potential amino acid residues that are involved in the formation of the active site [20, 21]. Despite these facts, empirical characterization of the active site of MVD has not been achieved, due to inherent difficulties in obtaining substrate - bound MVD.

In yeast, MVD is required for cell viability [14] and a mutation of leucine (Lue $_{79}$) to proline (Pro) (adjacent to the first cystein residue) of this enzyme has shown to confer temperature-sensitive phenotype of *S. cerevisiae* MN19-34 mutant [14]. The, pro-drug 6-fluoromevalonate and its derivatives (Fig. 1b) were reported as effective inhibitors of rat MVD [22, 23]. Although previous work on *S. cerevisiae* MVD led to the identification of certain active site amino acid residues which may be involved in the catalyses and substrate binding, their exact involvement in the enzyme activity and the formation of the transition state by ATP and MDP have not been fully investigated. Therefore the objectives of this study were to i) characterize the unknown active site of MVD to predict a probable reaction mechanism in the transition state. ii) unravel the effect of pro-drug 6-fluoromevalonate and its derivatives in MVD inhibition iii) study as to how mutation of Leu$_{79}$ and Pro confer temperature sensitivity in *S.cerevisiae* using a molecular docking and simulation-based approach.

Materials and methods

Sequence analysis

MVD sequences (Blastp e-value <4e–76) were retrieved from the non-redundant GenBank databases [http://blast.ncbi.nlm.nih.gov/Blast.cgi; 24] using the well-characterized MVD of *S. cerevisiae* (1FI4) [19] and the Blastp search tools of NCBI. Multiple alignments of retrieved amino acid sequences were carried out using CLUSTAL W of BioEdit version 5.0.6 (North Carolina State University, Department of Microbiology) and followed by manual refinement to maximize the similarity.

Molecular docking

The Cartesian coordinates of the x-ray crystal structure of *S. cerevisiae* MVD (1FI4) at 2.3 Å resolution [19] and ATP were retrieved from the PDB database [http://www.rcsb.org/pdb/home/home.do; 25] and HIC-Up [http://xray.bmc.uu.se/hicup/], respectively. Electronic structure calculation program Gaussian 98 was used to generate the Cartesian coordinates of enzyme substrate MDP, inhibitor triflouro mevalonatediposphate (TFMDP) and the protonated form of inhibitor at OH of the C3. Molecular graphics program Hex 4.2 [26] was employed for docking of ATP and MDP

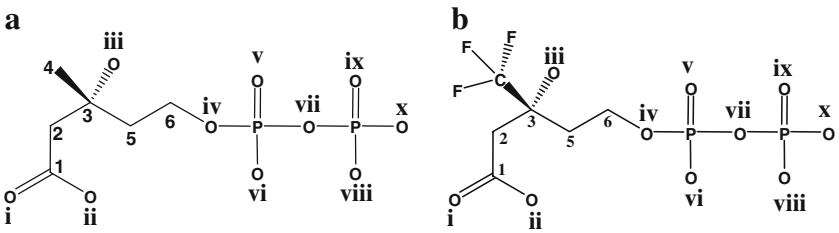

Fig. 1 Chemical structures showing positions of carbon (Arabic numerals) and oxygen (Roman numerals) in (**a**) mevalonate 5-diphosphate (MDP) and (**b**) triflouro mevalonatediphosphate (TFMDP)

and inhibitor with the protein. In brief, MDP and ATP were separately docked into putative regions (uniformly conserved in retrieved MVD sequences by multiple sequence alignment) of scMDD. Minimum binding score (MBS) for each docking was calculated by considering both the shape and electrostatic effect of the ligand. Since ATP bound to interdomain cleft of MVD had the highest MBS, MDP was docked into the close proximity ATP binding pocket. The MDP-ATP-MVD complex having the highest MBS (binding with highest negative values) was subjected to molecular dynamic simulation. Similarly, TFMDP and protonated TFMDP at hydroxyl of C3 were docked separately into unliganded MVD and the ATP-MVD and the complex with the highest MBS, were subjected to molecular dynamic simulation. All docking calculations were carried out by defining parameters at full rotation search mode, and correlation type of shape and electrostatics at receptor and ligand range of 180°, and twist range of 360°, grid of 0.6 with steric scan of 16 and final search of 25.

Molecular simulation

Four molecular dynamics simulations were carried out for substrate bound complex (MDP-ATP-MVD), inhibitor bound complex (TFMDP-MVD), mutated (Lue $_{79}$ → Pro) and the native MVD. Descriptions of the models taken for each simulation are given below.

Substrate bound complex

Cartesian coordinates of the MDP-ATP-MVD, were obtained from the docked configuration and subjected to molecular dynamics (MD) simulation. This complex was immersed in a rectangular box of dimensions of $15\times15\times13$ nm^3 and it was solvated by 8968 water molecules. Further 13 Na^+ ions were added by replacing randomly selected 13 water molecules from the system, to maintain electroneutrality of the system.

Inhibitor bound complex

The Cartesian coordinates of the TFMDP-MVD was taken from the same docking process as the initial structure for the MD simulation. This complex was also immersed in a box of water of the same size ($15\times15\times13$ nm^3). Electroneutrality of the system was maintained by adding 12 Na^+ ions by replacing randomly selected 12 water molecules from the box.

Mutated & native protein

The Lue$_{79}$ residue of *S. cerevisiae* MVD was substituted with Pro and the 3D structure of the mutated protein was constructed using Swiss Model, automated protein modelling server [http://swissmodel.expasy.org/SWISS-MODEL.html; 27]. The mutated structure was placed in the middle of a rectangular box of dimensions of $15\times15\times13$ nm^3 and was solvated by 9210 water molecules. To maintain electroneutrality, 8 Na^+ ions were added by replacing randomly selected 8 water molecules from the box. Identical conditions were also applied for native MVD.

Force fields

For water the SPC/E [28] model was used, while for ATP GROMOS96 ffG43a2 force field [29] was applied. Since for MVD and TFMVD there is no such standard force field the following protocol was applied to obtain a reasonable force field. Bond lengths, bond angles, dihedral angles and partial charges for MVD and TFMVD were taken from the structures of Gaussian98W [30] optimization with HF/6-31G (+) basis set. Potential parameters for non-bonded interactions and force constants were adopted from GROMOS96 ffG43a2 force field [29]. For the mutated protein and the original protein, the same GROMOS96 ffG43a2 force filed was employed.

Molecular dynamics simulation

All four systems, independently, were subjected to 100 steps of energy minimization using the steepest decent algorithm. This step was followed by 500 ps long molecular dynamics simulation while keeping the complexes / protein rigid. The purpose of the second step was to equilibrate the solvent (water) and the ions under the influence of the solute. After the second step, all four systems were simulated in the isothermal-isobaric ensemble at 300 K and 1 atm. The weak coupling technique [31] was used to modulate the temperature and pressure with relaxation times of 0.1 ps and 0.5 ps respectively. All bonds were constrained with LINCS [32] and relative tolerance of 10^{-4} nm, allowing 2 fs time step for the integration of the equations of motion. The particle mesh Ewald (PME) technique was used to evaluate electrostatic interactions [33, 34]. A real space convergence parameter of 3.5 nm^{-1} with the cutoff of 1.0 nm was used. The neighbor list was updated at every 10th step. Coordinates of all the atoms in all four systems were stored at every 0.5 ps and energy of the system was stored at every 0.1 ps for further analysis. It took about 64 hours for one simulation (1.5 ns long) on a single processor Pentium IV personal computer. All molecular dynamics simulations were carried out using GROMACS software package [35–37] and some of the analyses were carried out using the analysis modules in the same software package.

Results and discussion

Sequence analyses and rigid docking of substrates to enzyme

In a preliminary strategy towards the characterization of potential regions for active site of MVD, retrieved amino acid sequences of evolutionary diverse organisms were multiply- aligned (results not shown), revealing multiple conserved regions. Amongst MVDs in the PDB database, *S. cerevisiae* MVD (1FI4) being the structure with the highest resolution, interdomain cleft of the latter comprising conserved regions as revealed by multiple sequence alignment (see materials and methods) was targeted for substrates (ATP , MDP & TFMDP) docking. Figure 2 shows the results of docking and it revealed i) MDP did not bind to the interdomain cleft of the unliganded MVD ii) ATP binds to a region of the interdomain cleft ($R_{13–22}$: AYTFDAGPNAV) of unliganded MVD with a MBS of −387.88 iii) MDP binds to the $R_{13–22}$ region of an ATP liganded MVD with a MBS of −331.53 iv) Inhibitor TFMDP binds to a region of the interdomain cleft of ATP liganded MVD with a MBS of −215.16 and it binds towards the surface of the ATP and MDP binding cleft of unliganded (ATP unbound) MVD with a MBS of −378.19 (v) Protonated TFMDP at hydroxyl of C3 binds to the interdomain cleft of unliganded MVD with a MBS of −377.49. The binding pocket of ATP and MDP in *S. cerevisiae* MVD was found to be surrounded by in addition to conserved sequences of NIATLKYWGK (blue) at position 13–22, AYTFDAGPNAV (greenblue) at position 298–307 forming the lateral regions, two other regions, LASSAA (magenta) at position 115–121 forming the region on top and SGSA (green) of position 150–153 at the bottom (Fig. 2).

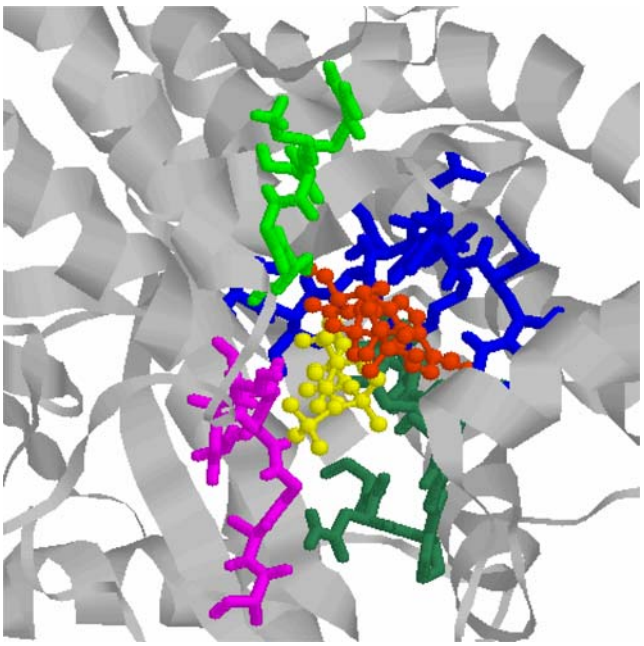

Fig. 2 Stereo view showing the relative positions of ATP (Red), MDP (Yellow) in putative active site of MVD following rigid docking with Hex 4.2. Putative active site amino acid residues of MVD are shown in coloured ball and sticks formats. Conserved amino acid sequences ($R_{13–22}$:NIATLKYWGK /Blue), ($R_{298–307}$:AYTFDAGPNAV /Green Blue), and ($R_{115–121}$: LASSAA /Magenta) and $R_{150–153}$ SGSA (Green)

Molecular dynamic simulation results

In docking the substrates and enzymes are considered as rigid molecules that cannot change their spatial arrangement in space during this process, however, in the real situation, the binding of substrates to enzymes is associated with conformational changes of respective molecules. To study these local and global conformational changes that may associate with the binding of substrate to enzymes, molecular dynamics (MD) simulation was implemented for the complex that resulted from docking. Similar approach has also been used in this study to investigate conformational changes that associate with mutated proteins. Given below are the results obtained from MD simulation of the docked molecules.

Root mean square deviation

Stability of the MDP-ATP-MVD and TFMDP-MVD complexes obtained from molecular dynamic simulations was examined by evaluating the root mean square deviations (RMSD) of all atoms of molecules, with respect to their initial configurations, as a function of the simulation time. Analyses of RMSD values of MVD in the complexes of MDP-ATP-MVD and TFMDP-MVD indicated MVD of the latter complex was relatively more stable, with lower RMSD fluctuations, compared to the MVD of the former complex (Fig. 3a and b). The RMSD profile of TFMDP does not show a considerable structural rearrangement over the entire simulation time after the initial increase of RMSD to about 0.17 nm while RMSD of MDP shows a considerable change during the simulation which may indicate structural rearrangements when the complex was exposed to the solvent environment. However, during the last part of the MD simulation of MDP-ATP-MVD complex RMSD did not show a larger change indicating a stable conformation of the substrate after the initial rearrangement. Even though the average of TFMDP RMSD (0.17±0.03 nm) is higher than that of MDP (0.135±0.008 nm) there was no significant change in the conformation over the entire simulation time after the initial rearrangement indicating a better binding of

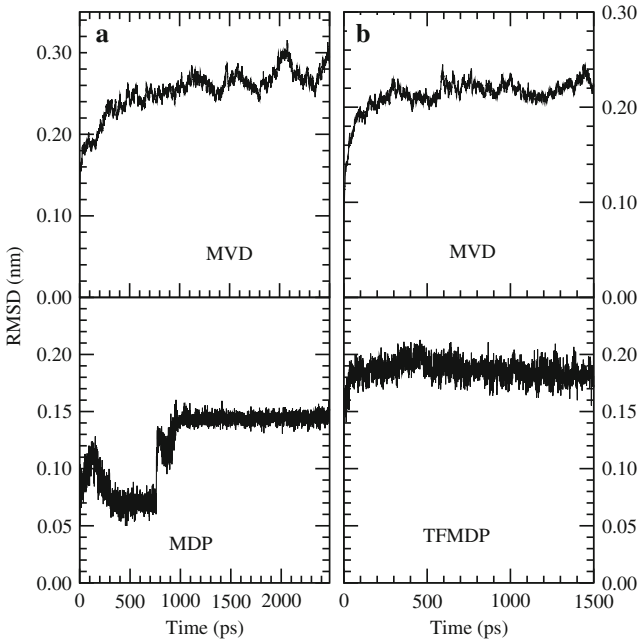

Fig. 3 Root mean square deviation (RMSD) of (**a**) MVD & MDP and (**b**) MVD & TFMDP with respect to their initial configurations as a function of simulation time

TFMDP to the binding sites of MVD. Superimposition of initial and final conformations of TFMDP and MDP following molecular dynamic simulations is given in Fig. 4.

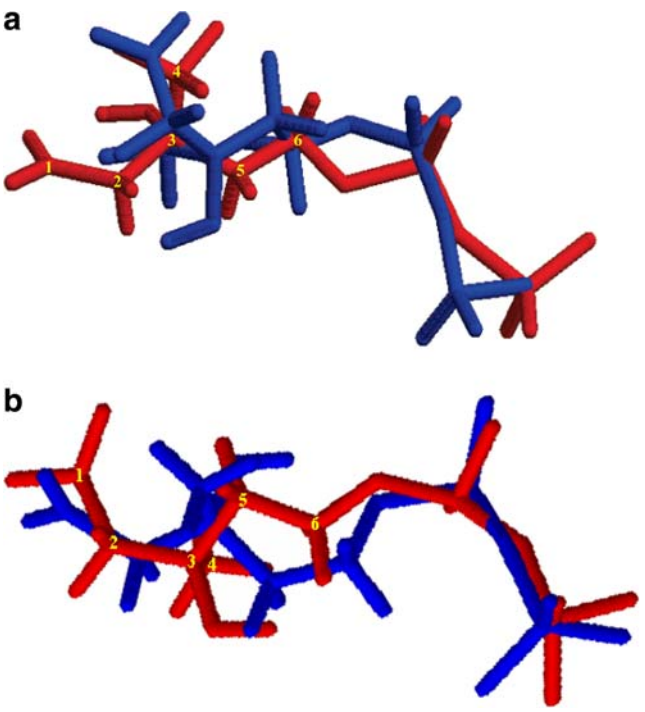

Fig. 4 Superimposition of initial (before molecular dynamic simulation/red) and final (after 1.5 ns long molecular dynamic simulation/blue) conformations of (**a**) TFMDP and (**b**) MDP

Interaction energy

Sum of the electrostatic energy and the dispersion energy between the MVD and MDP, and between MVD and TFMDP were calculated as a function of simulation time (Fig. 5). At the beginning of the simulation of the MVD-MDP complex, the interaction energy was around −350 kJ mol^{-1} and with progress of the simulation the energy becomes more negative and during the last 500 ps, interaction energy profile flattens out with an average energy of −608±74 kJ mol^{-1}. Interaction energy profile of MVD-TFMDP complex is always lower than that of MVD-MDP complex (Fig. 5) indicating better binding of the TFMDP to MVD compared to the binding of MDP to MVD.

Hydrogen bonds

The structure of MVD-ATP-MDP complex at the end of 1.5 ns long simulation was investigated to characterize active site residues of MVD. Criterion for this investigation was the interatomic distances of electronegative atoms in the complexes and distances ≤4 Å was considered as a potential distance for hydrogen bond formation. Analyses

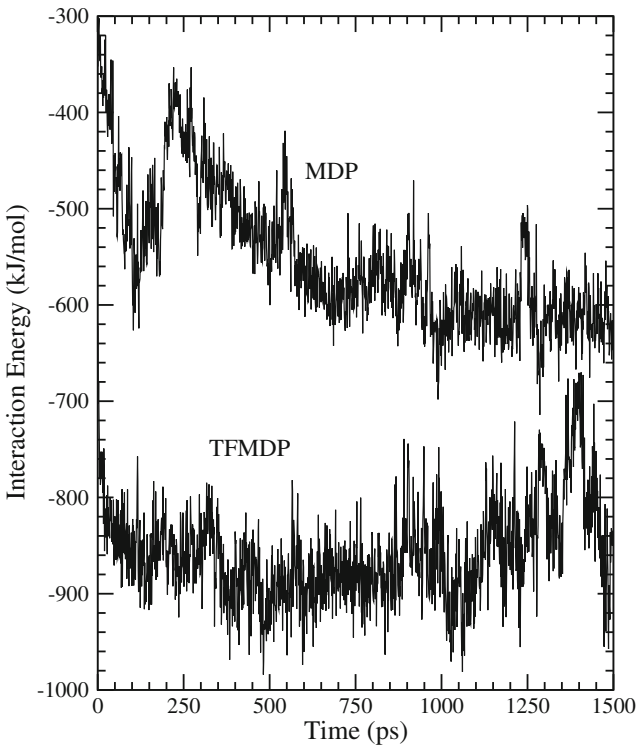

Fig. 5 Interaction energy (sum of the electrostatic energy and dispersion energy) between MVD & MDP and MVD & TFMDP as a function of the simulation time

revealed that N of Ala15, NZ of Lys18, OG of Ser121 and O of Ser155 of MVD are within hydrogen bond forming distances of O2, O2, O8 and O4 of MDP, respectively. Similar analyses with MVD-ATP revealed NZ of Lys22, OG of Ser153 & N of Ser155 of MVD to be within hydrogen bond forming distances of free O-P2, O-P3 & O-P1 of ATP, respectively. The distance profiles of these atomic pairs were calculated as a function of the simulation time which is then used to study the time at which hydrogen bonds are formed and stability of these hydrogen bonds. Figure 6a shows the results for MVD-MDP complex while Fig. 6b depicts the same for MVD-TFMDP complex (scale is given in the right side of the graph) and Fig. 7 gives the results for MVD-ATP complex. The distance profile of NZ of Lys18 with O2 of MDP indicated that this pair remains within hydrogen bond forming distance at the beginning and up to 100 ps and 900 ps to the end of the simulation time. In the same complex, (i) N of Ala15 and O2 of MDP were found to be in hydrogen bond forming distance in the entire simulation time except in the earlier part of the trajectory (ii) OG of Ser121 forms a stable hydrogen bond with O8 of MDP after the first 100 ps of the

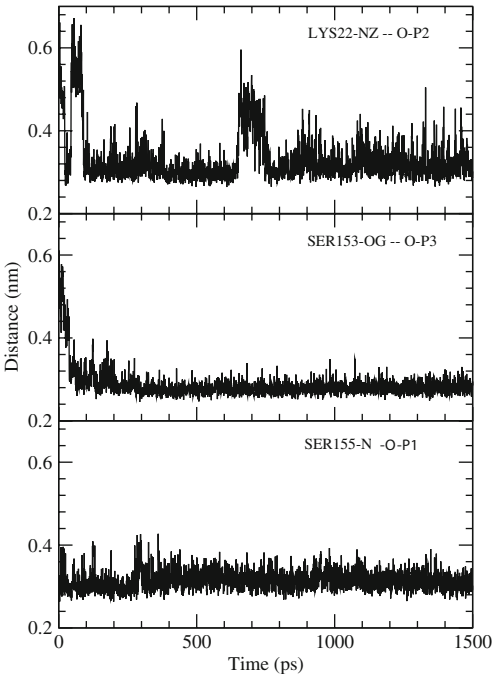

Fig. 7 Distance between atomic pairs of (**i**) NZ of Lys22 and O-P2 of ATP, (**ii**) OG of Ser153 and O-P3 of ATP and (**iii**) N of Ser155 and O-P1 of ATP as a function of simulation time

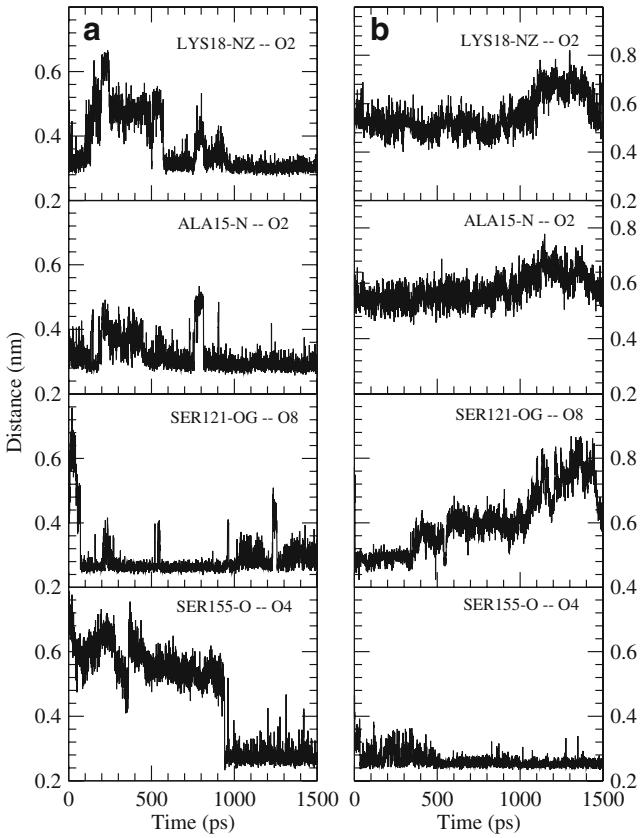

Fig. 6 Distances between possible hydrogen bond sites in (**a**) MVD-MDP complex and (**b**) the distances of the corresponding atomic pairs of MVD-TFMDP complex as a function of the simulation time

simulation despite the higher fluctuation in the hydrogen bond at the end of the trajectory (iii) O of Ser155 and O4 of MDP were seen to be within hydrogen bond forming distance after 900 ps. The investigation of distances between three atomic pairs of MVD-ATP that deemed to form H-bonds as a function of the simulation time revealed (i) the distance between NZ of Lys22 and O-P2 of ATP was greater than that of the typical hydrogen bond distance at the beginning and during the time period of 650 ps to 800 ps of the simulation, and it was shorter (~3 Å) than the hydrogen bond distance in the simulation range of 100 to 650 ps and 800 ps afterwards (Fig. 7), (ii) the distances between other atomic pairs, *i.e.* Ser153 & O-P3 and Ser155 & O-P1 of MVD-ATP complex were shorter than the hydrogen bond forming distance in the entire simulation period (Fig. 7).

Mutation analysis of Ser121 (S→A) has demonstrated the critical involvement of the latter residues in reaction catalysis [20]. In this study we found that OG of Ser121 and O8 of the MDP are within the hydrogen bond forming distance. Therefore we suggest that the reported catalytic activity of Ser121 may exert by binding of the latter residue with MDP through the formation of a hydrogen bond which may subsequently help in proper orienting of MDP either for phosphorylation or decarboxylation reaction or both reactions to take place. Further, mutation of Ser155 (S→A) has shown a 16-

fold inflation in K_m for MDP giving a clue to the possible involvement of this residue in MDP binding. Interestingly, in our study we found that O of Ser155 and O4 of the MDP are in hydrogen bond forming distance, strengthening the suggestion made by Krepkiy & Miziorko, 2005. Furthermore, the mutation of K18M resulted in a 30 fold decrease in activity and 16-fold inflation of the K_m for ATP suggesting that Lys18 influences the active site but is not crucial for reaction chemistry [20]. However, in our study we found that NZ of Lys18 and O2 of MDP, and NZ of Lys22 and O-P2 of ATP are in hydrogen bond forming distance. Therefore the empirical investigations to study the role of Lys18 with MDP, and Lys22 of ATP in the reaction are warranted. By mutation analyses of the invariant Ser residue of MVD to Ala [20] assigned a substrate binding function for Ser153 and Ser155 and the findings of our study indicated that these Ser residues of MVD are in within the hydrogen bond forming distance of ATP strengthening the suggestion made by Krepkiy & Miziorko [21].

Atomic pairs that deemed to form H-bonds in the MDP-MVD complex were sought in the MVD-TFMDP complex. This investigation revealed that there are no hydrogen bonds between NZ of Lys18 and O2 of the inhibitor, N of Ala15 and O2 of the inhibitor, OG of Ser121 and O8 of the inhibitor (Fig. 6b) and there is a very stable hydrogen bond between O of Ser155 with O4 of the inhibitor. These results suggest that there are four hydrogen bonds in MDP-MVD complex while only one hydrogen bond in MVD-TFMDP complex. However, according to the energy calculation (Fig. 5), it was revealed that there should be more than one hydrogen bond between the protein and the inhibitor. Therefore the final structure of the protein-TFMDP complex (or inhibitor-bound complex) was also investigated for possible hydrogen bonds using the criterion described elsewhere. The atomic pair, O of Ser155 of MVD and O4 of TFMDP, which were shown to form a H-bond in the previous analysis was ignored. Such analyses revealed OG of Tyr19, OG of Ser121, OG of Ser153, N of Gly154 and OG of Thr209 of MVD are within hydrogen bond forming distances of O5, O4, O7, O7 and O8 of the inhibitor, respectively. These atomic pairs were then subjected to the distance profiles calculation over the simulation time and the same calculation was also carried out for the corresponding atomic pairs of MVD-MDP complex for comparison. The results for the MVD-MDP and MVD-TFMDP complexes are presented in Fig. 8a and b, respectively. The investigation of inter atomic distances indicated that the hydrogen bond between (i) OG of Tyr19 of MVD and O5 of the TFMDP was very stable and it stayed intact throughout the entire simulation time (ii) OG of Ser121 of MVD and O4 of TFMDP formed after 400 ps and it stayed intact until

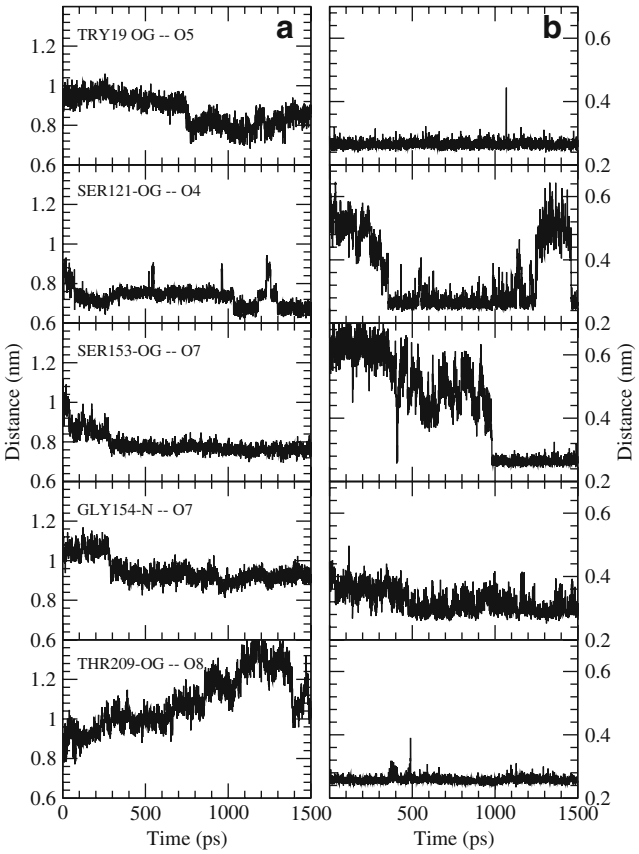

Fig. 8 Distance between possible hydrogen bond sites in (**b**) protein inhibitor complex (MVD-TFMDP) and (**a**) the distances of the corresponding atomic pairs of protein-substrate complex (MVD-ATP-MDP) as a function of the simulation time

1250 ps (iii) OG of Ser153 of MVD and O7 of TFMDF formed in the last 500 ps of the simulation (iv) N of Gly154 of MVD and O7 of TFMDP formed during the last 1000 ps (During the first 500 ps of the simulation, this distance fluctuates around 4 Å and it settles to an average of 3 Å at 500 ps and remains in this value till the end of the simulation) (v) OG of Thr209 of MVD and O8 of TFMDP was stable with a very low fluctuation. Interestingly, none of the corresponding atomic pairs in the MVD-MDP complex Fig. 8a show a propensity to form hydrogen bonds.

Catalytic activity of Asp 302

A previous study assigned a crucial catalytic role for Asp 302 of yeast MVD in the decarboxylation of MDP [20]. Investigation of this residue in the final configuration of the MVD-ATP-MDP-water system revealed that there were two water molecules (water_01 and water_02) in the vicinity of the carboxyl group of Asp302 residue and the hydroxyl group attached to C3 of MDP (Fig. 9). The time profile of

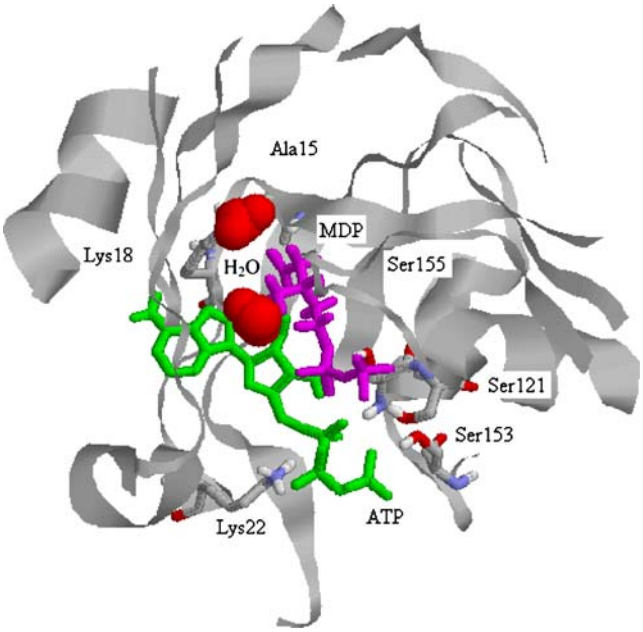

Fig. 9 Stereo view showing the relative positions of ATP, MDP, water molecules and amino acid residues of MVD in the putative active site of MVD, after 1.5 ns of molecular dynamics with GROMACS. MDP, ATP and water molecules are in magenta, green-blue and red colours respectively. Amino acid residues that are in the hydrogen bond forming distances with MDP (Ala15, Lys18, and Ser121 & Ser 155) and ATP (Lys 22, Ser153 & Ser 155) stick format. Active site was visualized with RasMol program

distances between the oxygen atoms of two water molecules and the oxygen of the hydroxyl group attached to C3 of MDP and the distances between the same two oxygen atoms of the above water molecules and an oxygen atom of the carboxyl group of Asp302 residue was calculated (Fig. 10). It is unequivocal that the water_01 molecule was not in the vicinity of either Asp302 or MDP at the beginning of the simulation. However, after about 350 ps of the dynamics, this water molecule has moved into the vicinity of the Asp302 residue and stays there till the end of the 2.5 ns long simulation. The other water molecule (water_02) was in the vicinity of Asp302 and MDP at the beginning of the simulation. Distances between these water molecules and MVD and MDP are in the range of 3 Å (about the hydrogen bond distance) in the last part of the trajectory showing greater affinity of MDP molecules towards the carboxyl group of Asp302 (Fig. 9). It is interesting to note that the two water molecules were alternatively forming hydrogen bonds with the carboxyl group of Asp302. Further, it can be seen that during the same time the distance between water-oxygen and the oxygen attached to C3 of MDP was fluctuating around about the hydrogen bond distance (Fig. 9). Phosphorylation of the C3 hydroxy of mevalonate diphosphate was proposed to be the early step of MVD catalyzed reaction [38]. Assignment of crucial catalytic base activity for Asp 302 that may deprotonate the C-3 hydroxyl of MDP suggests that these functional groups have to be closely juxtaposed in the MDP-ATP-MVD complex [20]. Finding two water molecules between carboxyl group of Asp302 and C3 region of MDP at a distance of 3 Å suggests that the reaction may proceed *via* a water molecule which may be deprotonated to OH^- which in turn may deprotonate the hydroxyl of C3.

Mutation of Leu_{79} to Pro

Mutation of Leu_{79} to Pro of *S. cerevisiae* MVD has been shown to confer temperature sensitive phenotype [14]. The effect of such a mutation was investigated using unliganded native 3D structures of MVD and its muted protein (Leu_{79}→Pro). In doing so both the latter structures were subjected to 1.5 ns long simulation and data obtained in the last 1.0 ns was analyzed. Root mean square deviations of both final structures with respect to their initial structures were calculated using a least square fitting procedure which fit final structures onto their initial structures. The all atom RMS deviation of MVD over 1.5 ns period is 0.247 nm while that for mutated MVD is 0.332 nm (Fig. 11). This

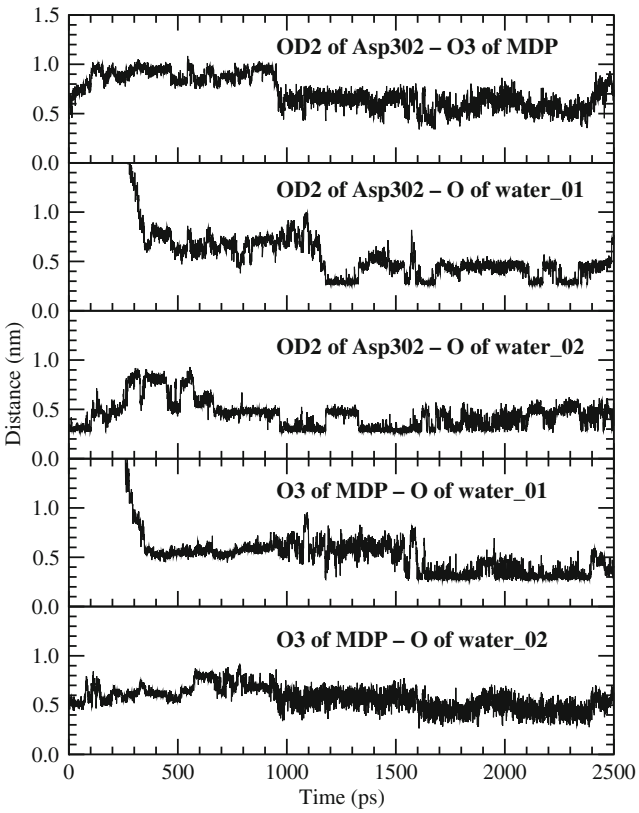

Fig. 10 Time profile of the distance between (**i**) OD2 of Asp 302 and O3 of MDP, (**ii**) OD2 of Asp 302 and O of water_01, (**iii**) OD2 of Asp302 and O of water_02, (**iv**) O3 of MDP and O of water_01 and (**v**) O3 of MDP and O of water_02

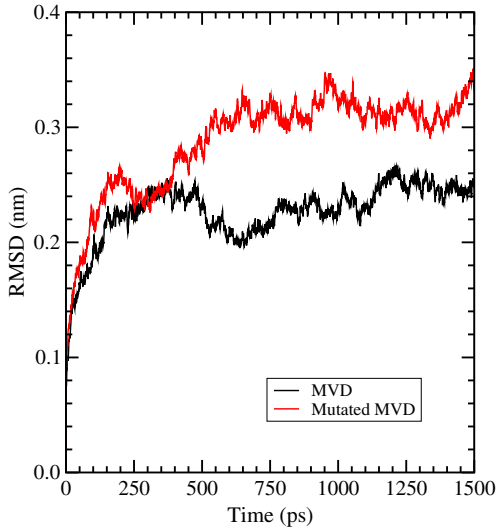

Fig. 11 RMS deviation of (**a**) MVD and (**b**) muted MVD after 1.5 ns molecular dynamics simulation at 300 K and at atmospheric pressure

indicates that there is a greater conformational change in the regions of Arg_{80} to Lys_{102} and Gly_{168} to Val_{178} of mutated MVD compared to native MVD from their initial structures. Further, root mean square deviations of the final structures (MVD and muted protein) with respect to their initial structures were compared visually by overlaying the final structures on their respective initial structures (Fig. 12). This also indicates the impact of the mutation on the conformational change of the mutated MVD. Therefore, it can be suggested that the temperature sensitive mutant phenotype of *S. cerevisiae* is a result of a significant conformational change associates with the Leu_{79} to Pro mutation.

Conclusions

In the current study, strictly conserved regions of MVD (NIATLKYW and AYTFDAGPNAV) that may bind with MDP and ATP were described, strengthening previous findings. In addition to active site residues reported previously, new residues, Ala15, and Lys 22, that binds with MDP and ATP, respectively were identified, warranting empirical investigations of the roles of these residues in the active site formation. Revelation of two water molecules between carboxyl group of Asp 302 and C3 region of MDP within hydrogen bond forming distance in 2.5 ns long simulation suggest that this reaction may proceed *via* a water molecule which may be deprotonated to OH^- which in turn may deprotonate the hydroxyl of C3. The assignment of crucial catalytic activity for Ser121 [20] and the findings reported in the current study, *i.e.* OG of Ser121 and O8 of the MDP are within hydrogen bond forming distance, suggest that the formation of a hydrogen bond subsequently helps in proper orienting of MDP either for phosphorylation or decarboxylation or both. Further, the finding that O of Ser155 and O4 of MDP are within hydrogen bond forming distance suggests that the observed drastic inflation of K_m reported following mutation of Ser 155 (S→A) [20] may have been due to the disruption of H-bond formation and hence MDP binding. Furthermore, assignment of substrate binding function for Ser153 and Ser155 by Krepkiy & Miziorko [20] has been proven in the current study by revealing the presence of latter residues in hydrogen bond forming distance with ATP. Finally, a significant conformational change associated with the Leu_{79} to Pro mutation of MVD compared to native MVD may have been the reason for the observed impaired activity of mutated MVD.

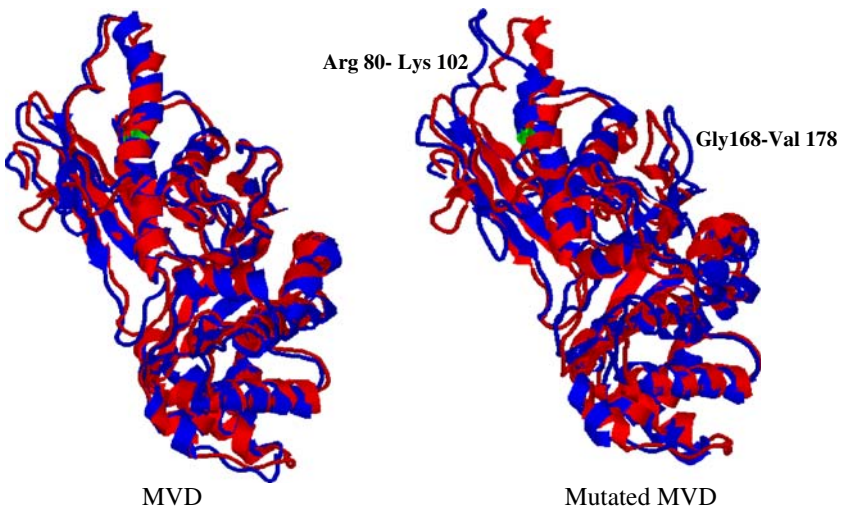

Fig. 12 Root mean square deviation of the final structure with respect to the initial structure of (**a**) MVD and (**b**) mutated MVD. Initial structures are given in red colour and the structures at the end of the simulation are given in blue colour. Both Leu_{79} and Pro are indicated in green colour. Regions of MVD that showed significant conformational changes following mutation and simulations are labelled

Acknowledgments We acknowledge the Department of Chemistry, University of Colombo, Sri Lanka for providing us with computer facilities and software for this work. We thank scientists who worked on MVD and published in scientific journals or deposited their data in publicly available databases. We further thank the scientists who developed Molecular Biology Software programs and Bioinformatics tools used in this study and also Dr. N.V. Chandrasekharan, Department of Chemistry, University of Colombo, Sri Lanka, for critical reading of the manuscript.

References

1. Rohmer M, Knani M, Simonin P, Sutter B, Sahm H (1993) Isoprenoid biosynthesis in bacteria: a novel pathway for the early steps leading to isopentenyl diphosphate. Biochem J 295:517–524
2. Edwards PA, Ericsson J (1999) Sterols and isoprenoids: signaling molecules derived from the cholesterol biosynthetic pathway. Annu Rev Biochem 68:157–185
3. Eisenreich W, Arigoni D, Bacher A, Rohdich F (2004) Biosynthesis of isoprenoids via the nonmevalonate pathway. Cell Mol Life Sci 6:1401–1426
4. Hunter WN (2007) Structure and reactivity in the non-mevalonate pathway of isoprenoid biosynthesis. J Biol Chem 282:21573–21577
5. Goldstein JL, Brown MS (1990) Regulation of the mevalonate pathway. Nature 343:425–430
6. Lichtenthaler H (1999) The 1-Deoxy-D-xylulose-5-phosphate pathway of isoprenoid biosynthesis in plants. Annu Rev Plant Physiol Plant Mol Biol 50:47–65
7. Rohmer M (1999) The discovery of a mevalonate-independent pathway for isoprenoid biosynthesis in bacteria, algae and higher plants. Nat Prod Rep 16:565–574
8. Rodriguez-Concepcion M, Boronat A (2002) Elucidation of the methylerythritol phosphate pathway for isoprenoid biosynthesis in bacteria and plastids. A metabolic milestone achieved through genomics. Plant Physiol 130:1079–1089
9. Bailey AM, Mahapatra S, Brennan PJ, Crick DC (2002) Identification, cloning, purification, and enzymatic characterization of Mycobacterium tuberculosis 1-deoxy-D-xylulose 5-phosphate synthase. Glycobiol 12:813–820
10. Chappell J (1995) Biochemistry and molecular biology of the isoprenoid biosynthetic pathway in plants. Annu Rev Plant Physiol Plant Mol Biol 46:521–547
11. Sacchettini JC, Poulter CD (1997) Creating isoprenoid diversity. Science 277:1788–1789
12. Rohmer M (1999) In: Barton D, Nakanishi K (eds) Comprehensive Natural Products Chemistry, vol 2. Elsevier , Amsterdam, pp 45–67
13. Kuzuyama T, Seto H (2003) Diversity of the biosynthesis of the isoprene units. Nat Prod Rep 20:171–183
14. Berges T, Guyonnet D, Karst F (1997) Characterisation of a Leu-to- Pro mutation in a conserved sequence of mevalonate diphosphate decarboxylase in yeast. J Bacteriol 179:4664–4670
15. Jabalquinto AM, Alvear ME, Cardemil E (1988) Physiological aspects and mechanism of action of mevalonate 5-diphosphate decarboxylase. Comp Biochem Physiol 9OB:671–677
16. Byres E, Alphey MS, Smith TK, Hunter WN (2007) Crystal structures of Trypanosoma brucei and Staphylococcus aureus mevalonate diphosphate decarboxylase inform on the determinants of specificity and reactivity. J Mol Biol 371:540–553
17. Dassanayake RS, Cao L, Samaranayake LP, Berges T (2002) Characterization, heterologous expression and functional analysis of mevalonate diphosphate decarboxylase gene (MVD) of *Candida albicans*. Mol Genet Genomics 267:281–290
18. Cordier H, Karst F, Berges T (1999) Heterologous expression in *Saccharomyces cerevisiae* of an *Arabidopsis thaliana* cDNA encoding mevalonate diphosphate decarboxylase. Plant Mol Biol 39:953–967
19. Bonanno JB, Edo C, Eswar N, Pieper U, Romanowski MJ, Ilyin Y, Gerchman SE, Kycia H, Studier FW, Sali A et al (2001) Structural genomics of enzymes involved in sterol/isoprenoid biosynthesis. Proc Natl Acad Sci 98:12896–12901
20. Krepkiy D, Miziorko HM (2004) Identification of active site residues in mevalonate diphosphate decarboxylase: Implications for a family of phosphotransferases. Protein Science 13:1875–1881
21. Krepkiy DV, Miziorko HM (2005) Investigation of the functional contributions of invariant serine residues in yeast mevalonate diphosphate decarboxylase. Biochem 44:2671–2677
22. Reardon JE, Abeles RH (1987) Inhibition of cholesterol biosynthesis by fluorinated mevalonate analogues. Biochem 26:4717–4722
23. Castillo M, Martinez-Cayuela M, Zafra MF, Garcia-Peregrin F (1991) Effect of phenylalanine derivatives on the main regulatory enzymes of hepatic cholesterogenesis. Mol Cell Biochem 105:21–25
24. Altschul SF, Warren G, Webb M, Eugene WM, David JL (1990) Basic local alignment search tool. J Mol Biol 215:403–410
25. Berman HM, Westbrook J, Feng Z, Gilliland G, Bhat TN, Weissig H, Shindyalov IN, Bourne PE (2000) The protein data bank. Nucl Acid Res 28:235–242
26. Mustard D, Ritchie DW (2005) Docking essential dynamics eigenstructure. Proteins 60:269–274
27. Arnold K, Bordoli L, Kopp J, Schwede T (2006) The SWISS-MODEL workspace: a web-based environment for protein structure homology modeling. Bioinformatics 22:195–201
28. Berensdsen HJC, Grigera JR, Straatma TP (1987) The missing term in effective pair potentials. J Phys Chem 91:6269–6271
29. Scott WRP, Hunenberger PH, Tironi IG, Mark AE, Billeter SR, Fennen J, Torda AE, Huber T, Kruger P, van Gunsteren WF (1999) The GROMOS biomolecular simulation program package. J Phys Chem A 103:3596–3607
30. Frisch MJ, Trucks GW, Schlegel HB, Scuseria GE, Robb MA et al (1998) Gaussian Inc, Pittsburgh PA
31. Berendsen HJC, Postma JPM, van Gunsteren WF, DiNola A, Haak JR (1984) Molecular dynamics with coupling to an external bath. J Chem Phys 81:3684–3690
32. Hess B, Bekker H, Berendsen HJC, Fraaije JGEM (1997) LINCS: a linear constraint solver for molecular simulations. J Comput Chem 18:1463–1472
33. de Leeuw SW, Perram JW, Smith ER (1980) Simulation of electrostatic systems in periodic boundary conditions. I. Lattice sums and dielectric constants. Proc R Soc London, Ser A 373:27–56
34. Darden T, York D, Pedersen LJ (1993) Particle mesh Ewald: An N log (N) method for Ewald sums in large systems. J Chem Phys 98:10089–10092
35. van der Spoel D, Lindahl E, Hess B, Groenhof G, Mark AE, Berendsen HJC (2005) GROMACS: fast, flexible and free. J Comp Chem 26:1701–1719
36. Berendsen HJC, van der Spoel D, van Drunen R (1995) GROMACS: a message-passing parallel molecular dynamics implementation. Comp Phys Comm 91:43–56
37. Lindahl E, Hess B, van der Spoel D (2001) Package for molecular simulation and trajectory analysis. J Mol Mod 7:306–317
38. Dhe-Paganon S, Magrath J, Abeles RJ (1994) Mechanism of mevalonate pyrophosphate decarboxylase: evidence for a carbocationic transition state. Biochem 33:13355–13362